# A DRIVER LINAC FOR THE ADVANCED EXOTIC BEAM LABORATORY: PHYSICS DESIGN AND BEAM DYNAMICS SIMULATIONS *

B. Mustapha†, P.N. Ostroumov and J.A. Nolen, ANL, Argonne, IL 60439, USA

*Abstract*

The Advanced Exotic Beam Laboratory (AEBL) being developed at ANL consists of an 833 MV heavy-ion driver linac capable of producing uranium ions up to 200 MeV/u and protons to 580 MeV with 400 kW beam power. We have designed all accelerator components including a two charge state LEBT, an RFQ, a MEBT, a superconducting linac, a stripper station and chicane. We present the results of an optimized linac design and end-to-end simulations including machine errors and detailed beam loss analysis.

## INTRODUCTION

The Advanced Exotic Beam Laboratory (AEBL) [1] has been proposed at ANL as a reduced scale of the original Rare Isotope Accelerator (RIA) project [2] with about half the cost but the same beam power. AEBL will address 90% or more of RIA physics but with reduced multi-users capabilities. The focus of this paper is the physics design and beam dynamics simulations of the AEBL driver linac. The reported results are for a multiple charge state $U^{238}$ beam.

## AEBL DRIVER LINAC

The proposed AEBL driver linac is an 833 MV superconducting CW machine capable of accelerating all ions from uranium (up to 200 MeV/u) to protons (up to 580 MeV). Figure 1 is a schematic layout of the proposed linac.

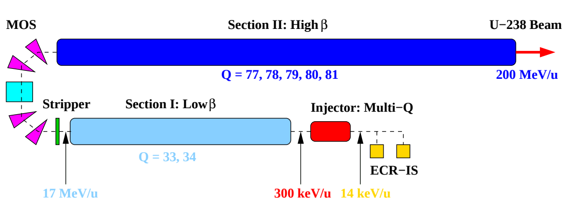


Figure 1: Schematic layout of the AEBL driver linac. For a uranium beam, two charge states ($33^+$,$34^+$) are accelerated from the ion source to a stripping station at 17 MeV/u after which five charge states ($77^+$,$78^+$,$79^+$,$80^+$,$81^+$) are accelerated in the high-$\beta$ section up to 200 MeV/u.

Table 1 presents the SC configuration of the linac.

Table 1: SC cavities types and properties. A total of 206 cavities: 72 in the low-$\beta$ section and 134 in the high-$\beta$ section. Cavity types are; FK: Fork, QW: Quarter-Wave, HW: Half-Wave, DS: Double-Spoke and TS: Triple-Spoke.

| Cav Type | F Mhz | L cm | $E_s$ MV/m | $E_a$ MV/m | # Cav |
|---|---|---|---|---|---|
| FK | 57.5 | 25 | 22.4 | 5.6 | 3 |
| QW | 57.5 | 20 | 27.5 | 9.29 | 21 |
| QW | 115.0 | 25 | 27.5 | 8.68 | 48 |
| HW | 172.5 | 30 | 27.5 | 9.45 | 40 |
| DS | 345.0 | 38.1 | 27.5 | 9.17 | 16 |
| TS | 345.0 | 65.2 | 27.5 | 9.55 | 54 |
| TS | 345.0 | 80.9 | 27.5 | 9.26 | 24 |

## LINAC DESIGN OPTIMIZATION

### *Multi-Q Injector: Two Options Investigated*

For the multi-q injector, we have investigated two possible options. A first option with LEBT-RFQ-MEBT and a second with LEBT-MHB-RFQ-MEBT where a multi-harmonic buncher is added in front of the RFQ. Figure 2 shows the longitudinal phase space plot for both options. We clearly see that the case with MHB produces a much smaller longitudinal emittance (about 8 times) than the case without MHB. Despite a 20% loss in the RFQ, the smaller longitudinal emittance obtained by pre-bunching makes the injection much smoother and reduces the risk of beam loss after the stripper as suggested by our previous studies [3]. A multi-q injector with MHB is adopted for AEBL driver.

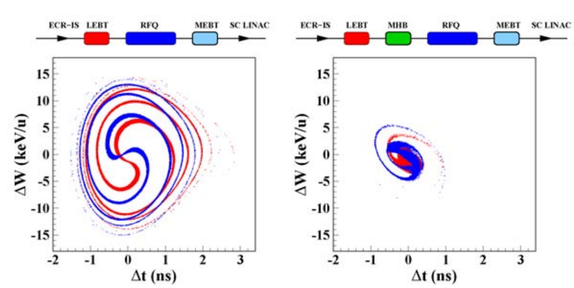


Figure 2: Longitudinal phase space plot a the end of a multi-q injector without (left) and with (right) a MHB.

### *Low Energy Section: Space Charge Effects*

The high beam power requirements (400 kW) means a relatively high beam current in the linac. Therefore space charge effects should be considered especially in the low-$\beta$

* This work was supported by the U.S. Department of Energy, Office of Nuclear Physics, under Contract No. DE-AC-02-06CH11357.
† mustapha@phy.anl.gov

section. Figure 3 shows the rms beam sizes for a uranium beam of 0.0 and 0.4 mA beam current. We may conclude that space charge effects are relatively minor for uranium and other heavy-ion beams. They may however play a more important role for proton and light-ion beams.

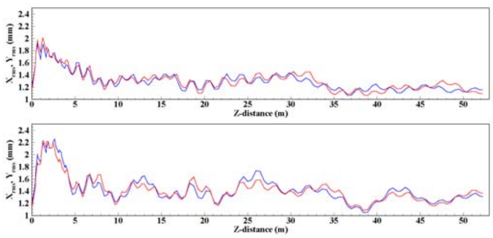


Figure 3: RMS beam sizes along the low-$\beta$ section for 0 mA (top) and 0.4 mA (bottom) mutli-q uranium beam.

### *Chicane: Matching and Collimation*

The chicane is a magnetic optical system following the stripper. In our case it is a symmetric $180^o$ bend with quadrupoles for matching, bending magnets, multipoles for higher order corrections and a RF buncher in the middle. Collimators to clean the beam and remove unwanted charge states are also included. Figure 4 shows the transverse acceptance of the chicane after optimizing the location and opening of the collimators (top) and the multi-q beam rms sizes along the chicane (bottom). The symmetry of the lattice is reflected on the beam for smooth matching to the high-$\beta$ section.

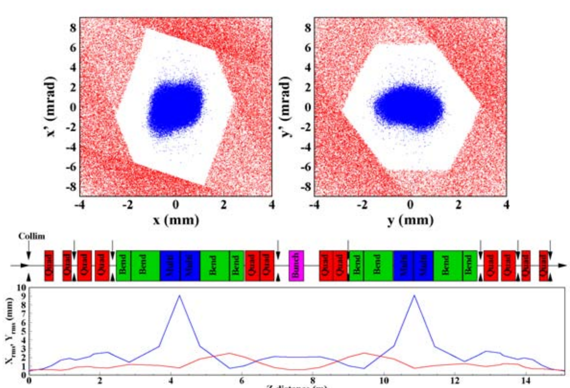


Figure 4: Acceptance of the chicane (top; red: acceptance limit, blue: real beam). Chicane lattice (middle) and RMS beam sizes (bottom; x:blue, y:red) along the chicane.

### *Multi-Q Beam Dynamics Optimization*

When accelerating multi-q beams, matching the lattice for the central charge state may not be enough to produce smooth beam dynamics. A better matching could be obtained by optimizing the lattice setting for the multi-q beam. The recent updates to the beam dynamics code TRACK [4] with the unique features of automatic longitudinal [5] and transverse [6] tuning of multi-q beams allowed faster and more accurate matching. Figure 5 shows the beam matched manually for the central charge state and the beam matched automatically for the multi-q beam. Such automatic beam tuning tools are essential for a multi-species machine like the AEBL driver linac.

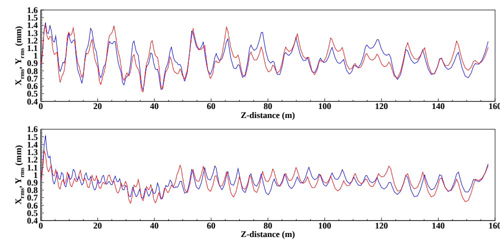


Figure 5: RMS beam sizes of a 5-q uranium beam along the high-$\beta$ section of the linac. Top: linac matched for central q. Bottom: linac matched automatically for the 5-q beam.

## BEAM DYNAMICS SIMULATIONS

Once the linac setting is optimized for the considered beam, end-to-end beam dynamics simulations including all sources of error are performed using TRACK [4].

### *Machine Error Simulations*

The main sources of error in the AEBL driver linac are element misalignments and the precision and stability of the RF system. The different errors as well as their typical values are listed in Table 2. In a given simulation, the actual errors are randomly generated according to the corresponding distribution. The uniform distributions are generated between the extreme values ± max. The Gaussian distributions are truncated at ± 3 rms value. The displacement errors are applied to the x and y positions of elements ends. The rotation errors are applied around the z axis (beam axis). For statistical significance the simulations were repeated 96 times starting every time from a different seed for the random number generator. $2 \times 10^5$ particles were tracked in every simulation. These large scale simulations were performed using the multi-seed parallel version of TRACK on the Jazz cluster at Argonne [7].

### *Results Before and After Corrections*

In order to asses the need for correctors especially transversely, we have simulated the case with and without transverse correctors using the errors in table 2. Figure 6 shows beam envelopes along the linac. We clearly see that before correction the envelopes exceed the beam pipe aperture in the high-$\beta$ section. After applying transverse corrections the envelopes are well within the aperture. Figure 7 shows beam 4×RMS emittances along the linac. We notice the significant reduction in the transverse emittances after applying the correctors. We conclude that transverse correc-

Table 2: Typical values of misalignment and RF errors.

| Error | Value | Distr. |
|---|---|---|
| Sol. end displacement<br>Short (20-25 cm)<br>Long 1(32-50 cm) | <br>0.15mm (max)<br>0.2 mm (max) | Uniform |
| Quad. end displacement | 0.15mm (max) | Uniform |
| Quad. rotation (z-axis) | 5 mrad (max) | Uniform |
| Cav. end displacement<br>Cav. field jitter error | 0.5 mm (max)<br>0.5 % (rms) | Uniform<br>Gaussian |
| Cav. phase jitter error | $0.5^o$(rms) | Gaussian |

tions are required especially in the chicane area before injecting the multi-q beam into the high-$\beta$ section.

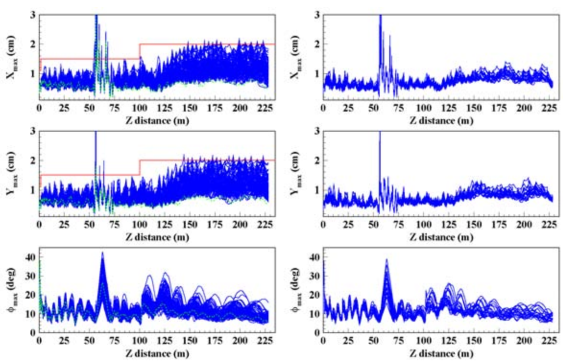

Figure 6: Beam envelopes along the linac for 96 seeds before (left) and after (right) transverse corrections. Green: ideal case without errors. Red: aperture limits.

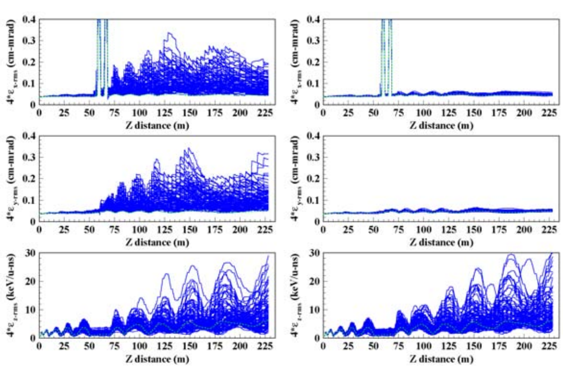

Figure 7: Beam 4×RMS emittances along the linac for 96 seeds before (left) and after (right) transverse corrections. Green: ideal case without errors.

### *Beam Loss Analysis*

Using TRACK allows to determine the exact location and fraction of any beam loss. Analyzing the output of TRACK for the case without corrections, we found 0% loss in the low-$\beta$ section, 8% loss in the chicane and 0.6 % loss in the high-$\beta$ section. After corrections there are no losses in both linac sections and the losses in the chicane are reduced to 0.06 %. Figure 8 shows the beam phase space plots at the end of the linac and the beam loss in Watts/m along the linac for both cases.

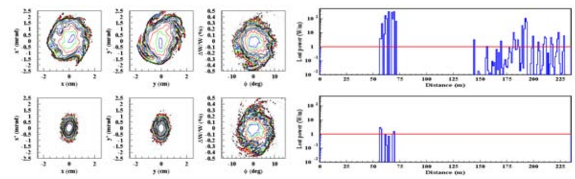

Figure 8: Left: Phase space plots without (top) and with corrections (bottom). Right: Beam loss in Watts/m along the linac without (top) and with corrections (bottom). The horizontal red line shows the conventional 1 W/m limit.

### *Larger Jitter Errors*

In order to further test the robustness of the actual AEBL linac design, we simulated two cases with larger RF fields phase and amplitude jitter errors while keeping misalignment errors at their values of table 2. In the ($1^o$,1%) case, $6\ 10^{-7}$ of the beam is lost in the low-$\beta$ section, $10^{-3}$ in the chicane and $2\ 10^{-6}$ in the high-$\beta$ section. The losses are amplified for ($2^o$,2%) to $2\ 10^{-5}$ in the low-$\beta$ section, $10^{-2}$ in the chicane and $2\ 10^{-3}$ in the high-$\beta$ section. Note that jitter of ($2^o$,2%) is a very extreme case. Figure 8 shows the beam phase space plots at the end of the linac and the beam loss in Watts/m along the linac for the three cases.

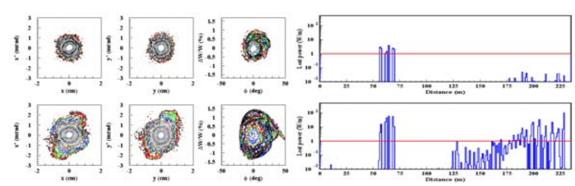

Figure 9: Left: Phase space plots for ($1^o$,1%) RF errors (top) and ($2^o$,2%) (bottom). Right: Beam loss in Watts/m along the linac for ($1^o$,1%) RF errors (top) and ($2^o$,2%) (bottom).

## REFERENCES

[1] P.N. Ostroumov et al, this conference, paper TUPAS005

[2] J.A. Nolen, Nucl. Phys. A734 (2004) 661.

[3] P.N. Ostroumov, V. N. Aseev, and B. Mustapha. Phys. Rev. ST. Accel. Beams 7, 090101 (2004).

[4] V.N. Aseev et al, Proceedings of PAC-05 Conference, Knoxville, Tennessee, May 16-20, 2005.

[5] B. Mustapha and P.N. Ostroumov, Phys. Rev. ST. Accel. Beams 8, 090101 (2005).

[6] B. Mustapha and P.N. Ostroumov, Proceedings of LINAC-06 Conference, Knoxville, Tennessee, Aug 21-25, 2006.

[7] Jazz web site: http://www.lcrc.anl.gov